PRE- AND POST-IMPACT INFLUENCES ON SCHRÖDINGER BASIN'S STRUCTURAL GEOLOGY.
Georgiana Y. Kramer[1], Teemu Öhman[1], Amanda L. Nahm[2], Patrick J. McGovern[1]; [1]Lunar Planet. Inst., Houston, TX, [2]Univ. Texas El Paso, El Paso, TX.

Introduction

Schrödinger Basin is 315 km in diameter and located at 75°S, 132.5°E, which places it on the western rim of the oldest and largest lunar basin, South Pole-Aitken (SPA). More precisely, Schrödinger is nestled between SPA's outer, modified final rim and inner, transient rim [1, 2]. Schrödinger is one of the youngest lunar basins, only marginally older than Orientale [3, 4]. It has been targeted as an ideal location for a future mission [5] because it contains materials associated with the SPA basin-forming event, ejected lithologies from the Orientale event, and experienced volcanism that occurred well after the main period of mare volcanism on the Moon.

We have been studying Schrödinger through a collaborative effort that brings together our different expertise in spectroscopy, petrology, photogeology, geophysics, structural geology, and impact cratering mechanics to fully characterize the geology and history of this singular region. Data sets used for this study include the Lunar Reconnaissance Orbiter (LRO) Wide Angle Camera (WAC) and Narrow Angle Camera (NAC) images, topography from LRO's Lunar Orbiter Laser Altimeter (LOLA), and spectral data from Chandrayaan-1's Moon Mineralogy Mapper (M^3).

Intra-Schrödinger Observations

Schrödinger hosts a series of fractures, which exhibit complex cross-cutting relationships with each other and with the basin floor materials, thereby offering clues about the timing of their formation.

Wide graben are 1 to 5 km wide, ~5 to 100 km long, and are curvilinear along their length. They occur mainly inside the peak ring, though in places they occur between the basin wall and the peak ring. Their formation is the result of faulting along antithetic pairs of normal faults. In places these structures widen as they cut across the peak ring, indicating that the underlying faults are deep. The width of these structures tends to decrease along length, indicating that the stresses decayed with length. These structures display an approximately basin-radial orientation in the S and SW.

Narrow graben are ~200 to 500 m wide, ~3 to 50 km long, are fairly linear, and display essentially constant width along their length. They occur primarily outside the peak ring. Pairs of narrow graben are generally orthogonal; the majority of these structures is concentric to the basin. The width of these structures implies shallower faulting compared to the wide graben. These structures may cut thin impact melt deposits in the basin interior.

Fractures or *lineations* tend to be isolated, i.e., they do not occur in pairs like the previous two structure classes, and are fairly linear.

The bluff is a relatively flat-topped, oblong, topographic high, ~22 km long, ~4 km wide, and ~170 m high near the center of Schrödinger. The bluff is attached to a low, east-facing, curvilinear scarp that trends generally north-south for ~55 km. The asymmetry in the scarp (i.e., the fact that the scarp faces one direction and is not a linear ridge) suggests the bluff may be a wrinkle ridge, which is the result of folding above a blind (non-surface cutting) thrust fault [6]. This interpretation is distinctly different from that of [4] and [7].

Some of these fractures are evidence of deep faulting associated with the formation of the basin. The possible exception is an orthogonal system of fractures in the southern basin floor outside of the peak ring, which may be related to Schrödinger's late-onset volcanism. One of these large fractures, which trends NE-SW, is possibly a graben formed as the result of faulting related to intrusion of the dike that fed Schrödinger's pyroclastic vent [8]. We are currently investigating whether this system of fractures is associated with the formation of the basin, and the altered stress states provided pathways ideally suited for magma ascent, or whether an expanding magma chamber once resided in this location, uplifted the basin floor, and formed the orthogonal fractures.

Extra-Schrödinger Observations

Analysis of the Schrödinger region utilizing WAC imagery and LOLA topography reveals several large impacts that occurred between the SPA and Schrödinger events (Fig. 1). Our fit of the location of these ancient crater rims is based primarily on LOLA topography, and supported by WAC imagery.

In Figure 1 it can be seen that four ancient craters lie concentric to Schrödinger's rim from the west to the north. These ancient craters actually abut the rim of Schrödinger, and probably explain why the rim of Schrödinger is so prominent in this location. Schrödinger's wall from the N to W is ~8 km high, and has an average slope of 15° from rim crest to basin floor. We interpret this as resulting from Schrödinger's rim being built upon the already elevated topography of the four concentrically aligned ancient crater rim pictured in Fig 1a (excluding Amundsen-Ganswindt). In contrast, the eastern rim is subdued compared to N

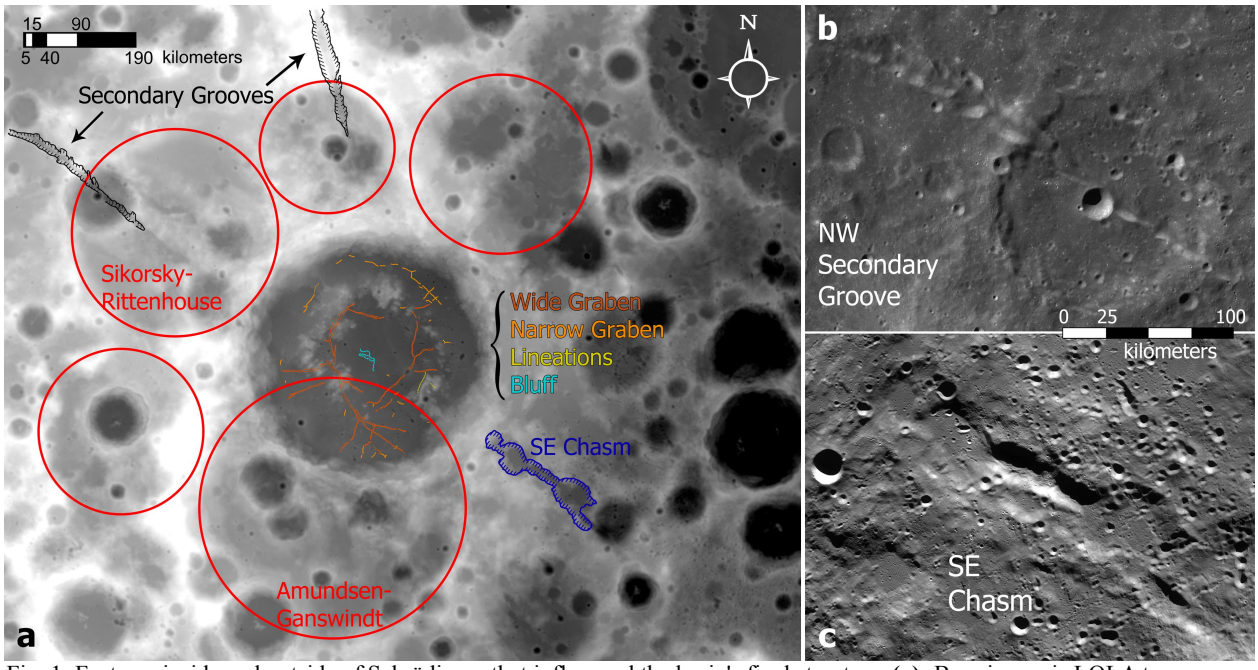

Fig. 1: Features inside and outside of Schrödinger that influenced the basin's final structure. **(a):** Base image is LOLA topography, from 256 m/pixel DEM. Red circles = ancient basins and craters that predate Schrödinger. Named basins indicate that they have been previously identified [3, 9]. See text for description of other features. **(b):** WAC image of Schrödinger's NW secondary groove - Vallis Schrödinger, exhibits classic crater chain morphology [10]. Compare to the SE Chasm **(c)**, which resembles a large graben.

and W with an average slope of only 2.3°. The rim of SPA and decreasing topography are the likely cause of Schrödinger's less prominent eastern rim.

The rim of the ancient basin Amundsen-Ganswindt [3-5, 9] is coincident with a major structural and topographic anomaly in Schrödinger's peak ring, that is, the missing southern portion of the peak ring. We interpret this to be a result of the interference of Amundsen-Ganswindt's basin rim topography on the development of Schrödinger's peak ring.

Although mapped by previous workers as one of Schrödinger's three secondary grooves [3], several observations indicate that the SE groove, or chasm, does not exhibit the same morphological characteristics as the secondary grooves to the N and NW, and is therefore not a secondary groove. In fact there are several observation that indicate the SE Chasm has a structural origin:

1. It is shorter and wider than the secondary grooves.
2. It lacks the chevron pattern characteristic of secondary crater chains [10].
3. It has a flat-bottom floor.
4. Two massive wall slumps within Schrödinger Basin at 10 o'clock and 4 o'clock line up with the trend of the SE chasm.
5. The pyroclastic vent also falls along the same linear trend.
6. The trend of the SE Chasm is orthogonal to the direction of the dike that fed the pyroclastic vent.
7. The curved trend of the long, wide graben in the south, that cuts Schrödinger's peak ring alludes to the influence on the regional stress field, at the time of its formation, from the SE Chasm.

All of these lines of evidence suggest that the orientation of these features is not coincidental. We are exploring the hypothesis that in these locations the structure of the wall was less stable, magma ascent was influenced by pre-existing structural discontinuities, and propagation of fractures followed a pre-established stress field resulting from the presence of a massive graben or fault (possibly related to SPA) that predated the Schrödinger impact.

Schrödinger presents a well-preserved example of a peak-ring crater whose formation was heavily influenced by pre-existing topography and tectonic structures, thus providing a key reference point for understanding cratering mechanics and verifying 3D numerical modeling results of crater formation in heterogeneous targets.

[1] Garrick-Bethell & Zuber (2009) *Science,* **323**; [2] Uemoto et al. (2011) *LPSC 42,* #1722; [3] Wilhelms (1987) *Geologic History of the Moon* [4] Shoemaker et al. (1994) *Science,* **266***;* [5] O'Sullivan et al. (2011) *GSA Spec. Paper 477,* 117-127; [6] Schultz (2000) *JGR,* **105**; [7] Mest (2011) *GSA Spec. Paper 477,* 95-115; [8] Kramer et al. (2011) *LPSC 42,* #1545; [9] Frey (2011) *GSA Spec. Paper 477,* 53-75; [10] Oberbeck & Morrison (1973) *Proc. LSC 4,* 107-123.